PLOS ONE

RESEARCH ARTICLE

# High versus low attenuation thresholds to determine the solid component of ground-glass opacity nodules

**Jae Ho Lee[1], Tae Hoon Kim[1], Sungsoo Lee[2], Kyunghwa Han[3], Min Kwang Byun[4], Yoon Soo Chang[4], Hyung Jung Kim[4], Geun Dong Lee[2☯¤]*, Chul Hwan Park[1☯]***

**1** Department of Radiology and the Research Institute of Radiological Science, Gangnam Severance Hospital, Yonsei University college of Medicine, Seoul, Republic of Korea, **2** Department of Thoracic and Cardiovascular Surgery, Gangnam Severance Hospital, Yonsei University college of Medicine, Seoul, Republic of Korea, **3** Department of Radiology, Research Institute of Radiological Science, Severance Hospital, Yonsei University College of Medicine, Seoul, Republic of Korea, **4** Division of Pulmonology, Department of Internal Medicine, Gangnam Severance Hospital, Yonsei University College of Medicine, Seoul, Republic of Korea

☯ These authors contributed equally to this work.
¤ Current address: Department of Thoracic and Cardiovascular Surgery, Asan Medical Center, University of Ulsan College of Medicine, Seoul, Republic of Korea
* geundy@hanmail.net (GDL); park_chulhwan@yuhs.ac (CHP)



OPEN ACCESS

**Citation:** Lee JH, Kim TH, Lee S, Han K, Byun MK, Chang YS, et al. (2018) High versus low attenuation thresholds to determine the solid component of ground-glass opacity nodules. PLoS ONE 13(10): e0205490. https://doi.org/10.1371/journal.pone.0205490

**Editor:** Aamir Ahmad, University of South Alabama Mitchell Cancer Institute, UNITED STATES

**Received:** October 20, 2017

**Accepted:** September 26, 2018

**Published:** October 18, 2018



**Data Availability Statement:** All relevant data are within the paper and its Supporting Information files.

**Funding:** The author(s) received no specific funding for this work.

**Competing interests:** The authors have declared that no competing interests exist.

**Abbreviations:** CT, computed tomography; GGN, ground-glass opacity nodules; HU, Hounsfield units; IA, invasive adenocarcinoma; MIA, minimally

## Abstract

### Objectives

To evaluate and compare the diagnostic accuracy of high versus low attenuation thresholds for determining the solid component of ground-glass opacity nodules (GGNs) for the differential diagnosis of adenocarcinoma in situ (AIS) from minimally invasive adenocarcinoma (MIA) and invasive adenocarcinoma (IA).

### Methods

Eighty-six pathologically confirmed GGNs < 3 cm observed in 86 patients (27 male, 59 female; mean age, 59.3 ± 11.0 years) between January 2013 and December 2015 were retrospectively included. The solid component of each GGN was defined using two different attenuation thresholds: high (-160 Hounsfield units [HU]) and low (-400 HU). According to the presence or absence of solid portions, each GGN was categorized as a pure GGN or part-solid GGN. Solid components were regarded as indicators of invasive foci, suggesting MIA or IA.

### Results

Among the 86 GGNs, there were 57 cases of IA, 19 of MIA, and 10 of AIS. Using the high attenuation threshold, 44 were categorized as pure GGNs and 42 as part-solid GGNs. Using the low attenuation threshold, 13 were categorized as pure GGNs and 73 as part-solid GGNs. The sensitivity, specificity, positive predictive value, negative predictive value, and diagnostic accuracy for the invasive focus were 55.2%, 100%, 100%, 22.7%, and 60.4%, respectively, for the high attenuation threshold, and 93.4%, 80%, 97.2%, 61.5%, and 91.8%, respectively, for the low attenuation threshold.

invasive adenocarcinoma; PPV, positive predictive value; NPV, negative predictive value.

## Conclusion

The low attenuation threshold was better than the conventional high attenuation threshold for determining the solid components of GGNs, which indicate invasive foci.

## Introduction

According to the new International Association for the Study of Lung Cancer/American Thoracic Society/European Respiratory Society lung adenocarcinoma classifications, adenocarcinoma is pathologically classified as a pre-invasive lesion (atypical adenomatous hyperplasia, adenocarcinoma in situ [AIS]), minimally invasive adenocarcinoma (MIA), or invasive adenocarcinoma (IA) according to the presence and size of the invasive foci [1]. Currently, adenocarcinoma is the most common histological type of lung cancer and often appears as ground-glass opacity nodules (GGNs) on computed tomography (CT) imaging [2].

GGNs are defined on CT as circumscribed lesions with hazy increased attenuation of the lung, but with preservation of the bronchial and vascular margins [3]. GGNs are subcategorized into pure and part-solid types, with part-solid nodules more likely to be primary lung cancer and associated with malignancy rates as high as 63% [4]. For the analysis of GGNs, the presence or absence and the size of the solid portion are important for differential diagnosis, determination of treatment strategy, and risk stratification [5–7]. Although the visual assessment method has been used to categorize GGNs in a few studies, the results have yielded only moderate inter-observer agreement [8–11].

Recently, a few studies have evaluated the utility of objective CT thresholds to determine the solid portion of GGNs [12–14]. These studies have used thresholds varying from -160 Hounsfield units (HU) to -350 HU; however, the optimal threshold for the solid portion of GGNs, which correspond to invasive foci in pathology, has not been established. Therefore, the aims of the present study were to evaluate and compare the diagnostic accuracy of high and low attenuation thresholds for the solid portion of GGN.

## Methods

The present study received approval from the institutional review board of Gangnam Severance Hospital (3-2016-0324). Clinical data were reviewed from medical records. Given the retrospective nature of the study and the use of anonymized data, requirements for informed consent were waived.

### Patients

Patients who underwent thoracic surgery between January 2013 and December 2015 due to persistent GGNs were enrolled and retrospectively reviewed. GGNs were defined as hazy areas of increased attenuation in the lung parenchyma with preserved bronchial and vascular markings on CT imaging. Patients who were diagnosed with AIS, MIA, or IA $< 3$ cm were included. Patients were excluded if the slice thickness of their pre-operative CT imaging was $> 2.5$ mm.

### CT protocol

CT scans were performed using one of two multi-detector scanners: a 16-slice (Somatom Sensation 16; Siemens Medical Solutions, Erlangen, Germany) or a 64-slice (Somatom Sensation 64; Siemens Medical Solutions, Erlangen, Germany) device. Scanning was performed during

inspiration in patients assuming a supine position. The scanning range was from apex of lung to adrenal gland. After obtaining a scout image to determine the field of view, conventional CT scanning was performed in the mediastinal window setting using a 1–2.5-mm reconstruction interval. The scanning parameters were as follows: voltage, 120 kVp; current, 100–200 mA; slice thickness 1–2.5 mm. CT images were reconstructed using the scanner's workstation. All CT images were retrieved from a picture archiving and communication system (Centricity 2.0, GE Medical Systems, Mt Prospect, IL, USA).

### CT image analysis

Two radiologists (C.H.P. and T.H.K), each with > 10 years of experience with chest radiology interpretation, assessed the CT images. All pre-operative CT images of the enrolled patients were transferred to a commercially available reconstruction program (Aquarius iNtuition Ver. 4.4.6 TeraRecon, Foster City, CA, USA), and then analyzed.

The solid component of GGNs was defined using two different attenuation thresholds: an area that demonstrated attenuation > -160 HU (high attenuation threshold); and an area that demonstrated attenuation > -400 HU (low attenuation threshold). After overlying the solid portion (above the threshold) using dedicated software, the radiologists manually outlined and segmented the solid portion. According to the presence or absence of a solid portion, GGNs were categorized into pure GGNs (no solid component) and part-solid GGNs (with solid component[s]) for each of the two thresholds. Solid components were considered to be indicators of invasive foci, suggesting MIA or IA (Fig 1).

### Statistical analysis

Continuous variables were summarized as mean ± SD, and categorical variables were summarized as frequencies or percentages. Data distributions were tested using the Shapiro-Wilk testThe sensitivity, specificity, positive predictive value (PPV), negative predictive value (NPV), and accuracy of the high and low attenuation threshold were calculated for the detection of invasive foci based on the assumption that the solid portion on CT images indicated invasive foci on pathology. Interobserver agreement regarding the presence or absence of solid portion was evaluated using Cohen kappa test. A kappa value of 0.00–0.20 indicated none to slight agreement; 0.21–0.40, fair agreement; 0.41–0.60, moderate agreement; 0.61–0.80, good agreement; and 0.81–1.00, excellent agreement. All statistical analyses were performed using commercially available software (SPSS version 20, IBM Corporation, Armonk, NY, USA) for Windows (Microsoft Corporation, Redmond, WA, USA) or SAS version 9.4 (SAS Institute Inc., Cary, NC, USA).

## Results

A total of 86 GGNs in 86 patients (27 male, 59 female; mean age 59.3 ± 11.0 years) were evaluated in this study. The mean size of the tumors was 15.0 ± 7.5 mm. Detailed demographic patient data are summarized in Table 1.

Among the 86 GGNs, there were 57 cases of IA, 19 of MIA, and 10 of AIS, which were pathologically confirmed in surgical specimens. Using the high attenuation threshold (-160 HU), 44 were categorized as pure GGNs (21 IA, 13 MIA, and 10 AIS), and 42 were categorized as part-solid GGNs (36 IA, 6 MIA and no AIS). With the low attenuation threshold (-400 HU), 13 were categorized as pure GGNs (3 IA, 2 MIA, and 8 AIS), and 73 as part-solid GGNs (54 IA, 17 MIA, and 2 AIS) (Table 2). The kappa values for the solid portion were 0.904 when using high attenuation threshold and 0.837 when using low attenuation threshold.

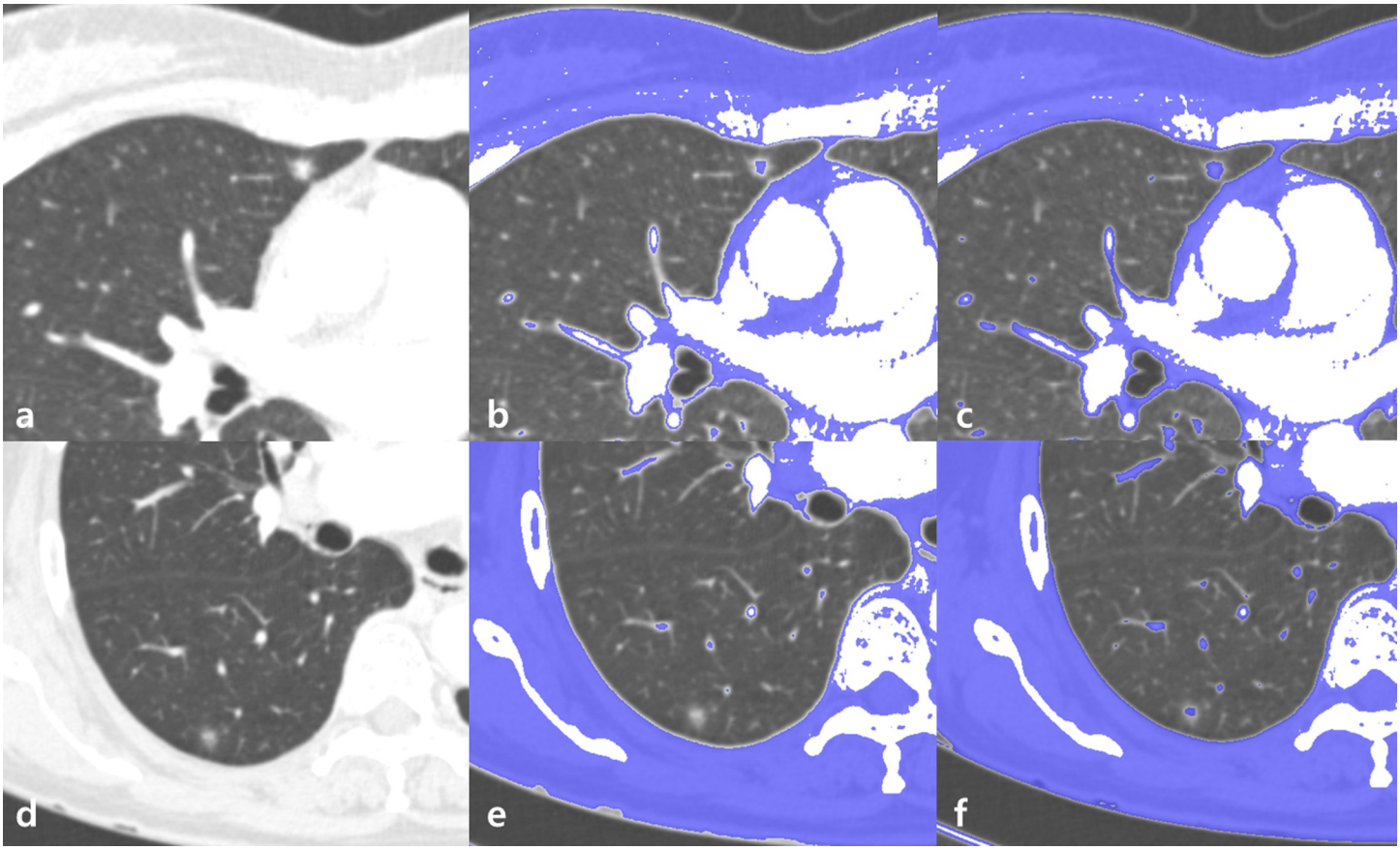


**Fig 1. Different subcategorization of ground-glass opacity nodules (GGNs) according to different thresholds: Classifying GGN according to two thresholds.** (a) Axial computed tomography (CT) image revealing GGN in the right middle lobe. (b) Axial CT images demonstrating areas above the high threshold (-160 Hounsfield units [HU]) (blue area). The GGN is identified as a part-solid GGN with a solid portion inside. (c) Axial CT images demonstrating areas above the low threshold (-400 HU) (blue area). The GGN is identified as a part-solid GGN with a solid portion inside. (d) Axial CT image demonstrating another GGN in the right lower lobe. (e) Axial CT images demonstrating areas above the high threshold (-160 HU) (blue area). The GGN is identified as a pure GGN without a solid portion inside. (f) Axial CT images demonstrating areas above the low threshold (-400 HU) (blue area). The GGN is identified as a part-solid GGN with a solid portion inside. As a result, the GGN in (a) is a part-solid GGN in both thresholds, whereas the GGN in (d) is a pure GGN in high threshold and part solid GGN in low threshold.

https://doi.org/10.1371/journal.pone.0205490.g001

The sensitivity, specificity, PPV, NPV, and diagnostic accuracy for the invasive foci were 55.2%, 100%, 100%, 22.7%, and 60.4%, respectively, using the high attenuation threshold, and 93.4%, 80%, 97.2%, 61.5%, and 91.8%, respectively, with the low attenuation threshold (Tables 3 and 4) [S1 File].

**Table 1. Demographic data of the 86 patients in this study.**

| Variables | AIS | MIA | IA |
|---|---|---|---|
| **Number (%)** | 10 (11.6%) | 19 (22.1%) | 57 (66.3%) |
| **Sex (male: female)** | 1:9 | 6:13 | 20:37 |
| **Age (years)** | 58.1 ± 9.6 | 57.0 ± 12.5 | 60.4 ± 10.8 |
| **Diameter (mm)** | 8.9 ± 3.8 | 10.1 ± 4.3 | 17.6 ± 7.4 |
| **Mean attenuation (HU)** | -611.9 ± 98.7 | -508.4 ± 76.2 | -404.8 ± 169.2 |

Data presented as mean ± SD unless otherwise indicated. AIS, adenocarcinoma in situ; MIA, minimally invasive adenocarcinoma; IA, invasive adenocarcinoma; HU Hounsfield units

https://doi.org/10.1371/journal.pone.0205490.t001

**Table 2. Sub-categorization of ground-glass opacity nodules (GGNs) according to high and low thresholds.**

| High attenuation threshold | | | Low attenuation threshold | | |
|---|---|---|---|---|---|
| **Pure GGN** | **AIS** | 10 (22.7%) | **Pure GGN** | **AIS** | 8 (61.5%) |
| | **MIA** | 13 (29.5%) | | **MIA** | 2 (15.4%) |
| | **IA** | 21 (47.8%) | | **IA** | 3 (23.1%) |
| | **Subtotal** | **44** | | **Subtotal** | **13** |
| **PS-GGN** | **AIS** | 0 (0%) | **PS-GGN** | **AIS** | 2 (2.7%) |
| | **MIA** | 6 (14.3%) | | **MIA** | 17 (23.3%) |
| | **IA** | 36 (85.7%) | | **IA** | 54 (74.0%) |
| | **Subtotal** | **42** | | **Subtotal** | **73** |

Data presented as n (%) unless otherwise indicated. AIS, adenocarcinoma in situ; MIA, minimally invasive adenocarcinoma; IA, invasive adenocarcinoma; PS, partly solid

https://doi.org/10.1371/journal.pone.0205490.t002

## Discussion

This study demonstrated that the low attenuation threshold (-400 HU) was better than the high attenuation threshold (-160 HU) in determining the solid component of GGNs, which indicates an invasive focus. GGNs can be divided into part-solid and pure according to morphology on CT imaging. Although the solid portions of GGNs have a tendency to represent invasive foci, they do not directly correspond with invasive foci [15]. Visual assessment with qualitative analysis for differential diagnosis of GGNs has well-known limitations, including inter-/intra-observer variations [11,16,17]. To overcome the drawbacks of visual assessments, various types of quantitative analysis of GGNs have recently been reported. The sizes of GGNs correlate with the invasion foci and pathologic results [18]. Lim et al. [19] reported that a difference in mean attenuation value could be observed between invasive and non-invasive adenocarcinomas. Lee et al. [20] suggested -472 HU as the cut-off of mean attenuation value in the evaluation of tumor invasiveness. However, with these methods, it is difficult to define the invasive focus of a GGN directly, although identifying the invasive focus is the easiest way to differentiate AIS from MIA and IA. Furthermore, in the 8$^{th}$ TNM guidelines the T staging of lung cancer depends on the size of the solid portion [21]. For these reasons, direct measurement of the solid portion of a GGN, which indicates an invasive focus, is crucial, and the absolute attenuation threshold to define invasive foci has been applied because CT attenuation is related to the density of the tissue [22]. Matsuguma et al. [12] attempted to define the solid portion of a GGN using a threshold of -160 HU. Ko et al. [13] set the threshold at -188 HU and regarded the part of the nodule that exhibited higher values as the solid component. Recently, Cohen et al [14] used -350 HU, as the threshold when measuring GGNs, because the invasive foci and solid component of the GGN demonstrated the highest agreement for that threshold. Therefore, the optimal threshold for identifying the solid portion of GGNs has not been established. In this study, we attempted to

**Table 3. Diagnostic accuracy of the high threshold for the detection of invasive foci on ground-glass opacity nodules (GGNs).**

| | IA + MIA | AIS | Total |
|---|---|---|---|
| **Pure GGN** | 34 | 10 | 44 |
| **Part solid GGN** | 42 | 0 | 42 |
| **Total** | 76 | 10 | 86 |

Data presented as n. AIS, adenocarcinoma in situ; MIA, minimally invasive adenocarcinoma; IA, invasive adenocarcinoma

https://doi.org/10.1371/journal.pone.0205490.t003

**Table 4. Diagnostic accuracy of the low threshold for the detection of invasive foci on ground-glass opacity nodules (GGNs).**

| | IA + MIA | AIS | Total |
|---|---|---|---|
| **Pure GGN** | 5 | 8 | 13 |
| **Part-solid GGN** | 71 | 2 | 73 |
| **Total** | 76 | 10 | 86 |

Data presented as n. AIS, adenocarcinoma in situ; MIA, minimally invasive adenocarcinoma; IA, invasive adenocarcinoma

https://doi.org/10.1371/journal.pone.0205490.t004

obtain better thresholds for defining the solid portion of GGNs. We used -400 HU as a representative low threshold and -160 HU as a representative high threshold. The high threshold categorized all AIS cases as pure GGNs, but 44.8% of MIA and IA cases were also categorized as pure GGNs. In contrast, with the low threshold, 93.4% of MIA and IA cases were categorized as part-solid GGNs. These findings suggest that with the use of a high threshold, invasive foci may be missed, and a low threshold might be better at distinguishing MIA and IA, which are observed as part-solid GGNs, from AIS, which are observed as pure GGNs.

With the development of CT technology and analysis software, advanced analyses are possible for differential diagnosis of GGNs. Recently, quantitative CT texture analysis has provided diverse potential applications for GGN differentials. Ikeda et al. [23] reported that IA exhibited two peaks on a CT histogram. Son et al. [24] demonstrated that the 75th percentile CT attenuation value could be used to distinguish IA from pre-invasive lesions. Kurtosis, skewness, or entropy of GGNs could be used for differentiating pre-invasive lesions and IA [24–26]. In addition, advanced radiomic features including shape and morphology metrics, Renyi dimensions, geometrical measures, and the gray-level co-occurrence matrix or the gray-level run length matrix might be useful for differential diagnosis of GGNs [27]. However, these complex methods are difficult to apply in daily practice, and further validation is needed [26].

Our study had some limitations, including its single-center, retrospective design and the small sample size. Second, vessels on CT imaging were not perfectly removed due to the limitations of manual image processing. Third, the slice thickness of CT images ranged from 1 mm to 2.5 mm, which may have led to a volume averaging effect in thicker sections of the CT scans [28,29]. Fourth, in most cases, one dedicated pathologist with experience in lung cancer reported the pathologic results, but in some cases, different pathologists with different expertise reported. Fifth, this study did not evaluate longitudinal changes of GGNs, although changes in CT characteristics, including density, are helpful for differential diagnosis [30]. In addition, in this study, attenuation thresholds of -160 HU and -400 HU were compared, but these are representative values of low and high thresholds, and since neither is likely to be the optimal threshold, further evaluation for determining the optimal threshold will be necessary.

In conclusion, a low attenuation threshold was better than a high attenuation threshold in determining the solid components of GGNs, which indicate invasive foci. Quantitative analysis using a low threshold for the solid portions of GGNs could be a simple and accurate method to define invasive foci.

## Supporting information

**S1 File. Attached file includes data of the pathogolic results in surgical specimens and subcategorizations of ground-glass opacity nodules according to high and low thresholds.**
(XLSX)

## Author Contributions

**Conceptualization:** Tae Hoon Kim, Geun Dong Lee, Chul Hwan Park.

**Data curation:** Kyunghwa Han, Chul Hwan Park.

**Formal analysis:** Jae Ho Lee, Tae Hoon Kim, Kyunghwa Han, Chul Hwan Park.

**Investigation:** Jae Ho Lee, Sungsoo Lee, Min Kwang Byun, Yoon Soo Chang, Hyung Jung Kim, Geun Dong Lee, Chul Hwan Park.

**Methodology:** Jae Ho Lee, Tae Hoon Kim, Sungsoo Lee, Kyunghwa Han, Min Kwang Byun, Yoon Soo Chang, Hyung Jung Kim, Chul Hwan Park.

**Supervision:** Tae Hoon Kim, Sungsoo Lee, Hyung Jung Kim.

**Writing – original draft:** Jae Ho Lee, Geun Dong Lee, Chul Hwan Park.

## References


1. Travis WD, Brambilla E, Noguchi M, Nicholson AG, Geisinger KR, Yatabe Y, et al. International association for the study of lung cancer/american thoracic society/european respiratory society international multidisciplinary classification of lung adenocarcinoma. J Thorac Oncol. 2011; 6: 244–285. https://doi.org/10.1097/JTO.0b013e318206a221 PMID: 21252716
2. Torre LA, Bray F, Siegel RL, Ferlay J, Lortet-Tieulent J, Jemal A. Global cancer statistics, 2012. CA Cancer J Clin. 2015; 65: 87–108. https://doi.org/10.3322/caac.21262 PMID: 25651787
3. Hansell DM, Bankier AA, MacMahon H, McLoud TC, Muller NL, Remy J. Fleischner Society: glossary of terms for thoracic imaging. Radiology. 2008; 246: 697–722. https://doi.org/10.1148/radiol.2462070712 PMID: 18195376
4. Henschke CI, Yankelevitz DF, Mirtcheva R, McGuinness G, McCauley D, Miettinen OS. CT screening for lung cancer: frequency and significance of part-solid and nonsolid nodules. AJR Am J Roentgenol. 2002; 178: 1053–1057. https://doi.org/10.2214/ajr.178.5.1781053 PMID: 11959700
5. MacMahon H, Naidich DP, Goo JM, Lee KS, Leung ANC, Mayo JR, et al. Guidelines for Management of Incidental Pulmonary Nodules Detected on CT Images: From the Fleischner Society 2017. Radiology. 2017; 284: 228–243. https://doi.org/10.1148/radiol.2017161659 PMID: 28240562
6. Heuvelmans MA, Oudkerk M. Management of subsolid pulmonary nodules in CT lung cancer screening. J Thorac Dis. 2015; 7: 1103–1106. https://doi.org/10.3978/j.issn.2072-1439.2015.07.23 PMID: 26380722
7. Naidich DP, Bankier AA, MacMahon H, Schaefer-Prokop CM, Pistolesi M, Goo JM, et al. Recommendations for the management of subsolid pulmonary nodules detected at CT: a statement from the Fleischner Society. Radiology. 2013; 266: 304–317. https://doi.org/10.1148/radiol.12120628 PMID: 23070270
8. Edge SB, Compton CC. The American Joint Committee on Cancer: the 7th edition of the AJCC cancer staging manual and the future of TNM. Ann Surg Oncol. 2010; 17: 1471–1474. https://doi.org/10.1245/s10434-010-0985-4 PMID: 20180029
9. Austin JH, Garg K, Aberle D, Yankelevitz D, Kuriyama K, Lee HJ, et al. Radiologic implications of the 2011 classification of adenocarcinoma of the lung. Radiology. 2013; 266: 62–71. https://doi.org/10.1148/radiol.12120240 PMID: 23070271
10. Revel MP, Bissery A, Bienvenu M, Aycard L, Lefort C, Frija G. Are two-dimensional CT measurements of small noncalcified pulmonary nodules reliable? Radiology. 2004; 231: 453–458. https://doi.org/10.1148/radiol.2312030167 PMID: 15128990
11. Kakinuma R, Ashizawa K, Kuriyama K, Fukushima A, Ishikawa H, Kamiya H, et al. Measurement of focal ground-glass opacity diameters on CT images: interobserver agreement in regard to identifying increases in the size of ground-glass opacities. Acad Radiol. 2012; 19: 389–394. https://doi.org/10.1016/j.acra.2011.12.002 PMID: 22222027
12. Matsuguma H, Nakahara R, Anraku M, Kondo T, Tsuura Y, Kamiyama Y, et al. Objective definition and measurement method of ground-glass opacity for planning limited resection in patients with clinical stage IA adenocarcinoma of the lung. Eur J Cardiothorac Surg. 2004; 25: 1102–1106. https://doi.org/10.1016/j.ejcts.2004.02.004 PMID: 15145016

13. Ko JP, Suh J, Ibidapo O, Escalon JG, Li J, Pass H, et al. Lung Adenocarcinoma: Correlation of Quantitative CT Findings with Pathologic Findings. Radiology. 2016; 280: 931–939. https://doi.org/10.1148/radiol.2016142975 PMID: 27097236

14. Cohen JG, Goo JM, Yoo RE, Park CM, Lee CH, van Ginneken B, et al. Software performance in segmenting ground-glass and solid components of subsolid nodules in pulmonary adenocarcinomas. Eur Radiol. 2016; 26: 4465–4474. https://doi.org/10.1007/s00330-016-4317-3 PMID: 27048527

15. Lee KH, Goo JM, Park SJ, Wi JY, Chung DH, Go H, et al. Correlation between the size of the solid component on thin-section CT and the invasive component on pathology in small lung adenocarcinomas manifesting as ground-glass nodules. J Thorac Oncol. 2014; 9: 74–82. https://doi.org/10.1097/JTO.0000000000000019 PMID: 24346095

16. Wormanns D, Diederich S, Lentschig MG, Winter F, Heindel W. Spiral CT of pulmonary nodules: interobserver variation in assessment of lesion size. Eur Radiol. 2000; 10: 710–713. https://doi.org/10.1007/s003300050990 PMID: 10823619

17. Zhao B, James LP, Moskowitz CS, Guo P, Ginsberg MS, Lefkowitz RA, et al. Evaluating variability in tumor measurements from same-day repeat CT scans of patients with non-small cell lung cancer. Radiology. 2009; 252: 263–272. https://doi.org/10.1148/radiol.2522081593 PMID: 19561260

18. Lee GD, Park CH, Park HS, Byun MK, Lee IJ, Kim TH, et al. Lung Adenocarcinoma Invasiveness Risk in Pure Ground-Glass Opacity Lung Nodules Smaller than 2 cm. Thorac Cardiovasc Surg. 2018. 2018/01/24. https://doi.org/10.1055/s-0037-1612615 PMID: 29359309

19. Lim HJ, Ahn S, Lee KS, Han J, Shim YM, Woo S, et al. Persistent pure ground-glass opacity lung nodules >/ = 10 mm in diameter at CT scan: histopathologic comparisons and prognostic implications. Chest. 2013; 144: 1291–1299. https://doi.org/10.1378/chest.12-2987 PMID: 23722583

20. Lee HY, Choi YL, Lee KS, Han J, Zo JI, Shim YM, et al. Pure ground-glass opacity neoplastic lung nodules: histopathology, imaging, and management. AJR Am J Roentgenol. 2014; 202: W224–233. https://doi.org/10.2214/AJR.13.11819 PMID: 24555618

21. Goldstraw P, Chansky K, Crowley J, Rami-Porta R, Asamura H, Eberhardt WE, et al. The IASLC Lung Cancer Staging Project: Proposals for Revision of the TNM Stage Groupings in the Forthcoming (Eighth) Edition of the TNM Classification for Lung Cancer. J Thorac Oncol. 2016; 11: 39–51. https://doi.org/10.1016/j.jtho.2015.09.009 PMID: 26762738

22. Gucuk A, Uyeturk U. Usefulness of hounsfield unit and density in the assessment and treatment of urinary stones. World J Nephrol. 2014; 3: 282–286. https://doi.org/10.5527/wjn.v3.i4.282 PMID: 25374823

23. Ikeda K, Awai K, Mori T, Kawanaka K, Yamashita Y, Nomori H. Differential diagnosis of ground-glass opacity nodules: CT number analysis by three-dimensional computerized quantification. Chest. 2007; 132: 984–990. https://doi.org/10.1378/chest.07-0793 PMID: 17573486

24. Son JY, Lee HY, Lee KS, Kim JH, Han J, Jeong JY, et al. Quantitative CT analysis of pulmonary ground-glass opacity nodules for the distinction of invasive adenocarcinoma from pre-invasive or minimally invasive adenocarcinoma. PLoS One. 2014; 9: e104066. https://doi.org/10.1371/journal.pone.0104066 PMID: 25102064

25. Chae HD, Park CM, Park SJ, Lee SM, Kim KG, Goo JM. Computerized texture analysis of persistent part-solid ground-glass nodules: differentiation of preinvasive lesions from invasive pulmonary adenocarcinomas. Radiology. 2014; 273: 285–293. https://doi.org/10.1148/radiol.14132187 PMID: 25102296

26. Cohen JG, Reymond E, Medici M, Lederlin M, Lantuejoul S, Laurent F, et al. CT-texture analysis of subsolid nodules for differentiating invasive from in-situ and minimally invasive lung adenocarcinoma subtypes. Diagn Interv Imaging. 2018; 99: 291–299. https://doi.org/10.1016/j.diii.2017.12.013 PMID: 29477490

27. Li W, Wang X, Zhang Y, Li X, Li Q, Ye Z. Radiomic analysis of pulmonary ground-glass opacity nodules for distinction of preinvasive lesions, invasive pulmonary adenocarcinoma and minimally invasive adenocarcinoma based on quantitative texture analysis of CT. Chin J Cancer Res. 2018; 30: 415–424. https://doi.org/10.21147/j.issn.1000-9604.2018.04.04 PMID: 30210221

28. Goo JM, Park CM, Lee HJ. Ground-glass nodules on chest CT as imaging biomarkers in the management of lung adenocarcinoma. AJR Am J Roentgenol. 2011; 196: 533–543. https://doi.org/10.2214/AJR.10.5813 PMID: 21343494

29. Collins J, Stern EJ. Ground-glass opacity at CT: the ABCs. AJR Am J Roentgenol. 1997; 169: 355–367. https://doi.org/10.2214/ajr.169.2.9242736 PMID: 9242736

30. Zhang YP, Heuvelmans MA, Zhang H, Oudkerk M, Zhang GX, Xie XQ. Changes in quantitative CT image features of ground-glass nodules in differentiating invasive pulmonary adenocarcinoma from benign and in situ lesions: histopathological comparisons. Clin Radiol. 2018; 73: 504.e509-504.e516.